International Conference
Nuclear Energy for New Europe

Experimental Investigation of Taylor Bubble Decay Rate in Counter-current Flow

Žiga Perne
Reactor Engineering Division
Jožef Stefan Institute
1000, Ljubljana, Slovenia
ziga.perne@gmail.com

Antoine Lamour, Blaž Mikuž
Reactor Engineering Division
Jožef Stefan Institute
1000, Ljubljana, Slovenia
antoine.lamour@etu.uca.fr, blaz.mikuz@ijs.si

ABSTRACT

During the loss of coolant accident (LOCA) in a pressure water reactor (PWR) the depressurization in the primary loop can cause boiling of cooling water and formation of large vapour slugs. In such event, Taylor bubbles may occur in the emergency core cooling system (ECCS) of a pressure water reactor (PWR) or in the U-pipes of a steam generator. In general, Taylor bubbles are unwanted in the primary loop of a PWR, thus, it is important to understand their behaviour in different fluids and flow conditions. We have investigated Taylor bubble decay rate in a vertical pipe with downward liquid flow in order to study the effects of the absolute pressure, temperature, bubble length and pipe diameter on the rate of bubble size reduction. For water-gas mixtures, it has been observed that a Taylor bubble disintegrates (i.e. decays in size) over time when exposed to a turbulent flow regime. The experiment was carried out in circular glass pipes with inner diameters of 12.4 and 26 mm, and 1.6 m in length. Temperature and absolute pressure were recorded at the top and bottom of the test section, and the pressure drop across the pipe was recorded using a differential pressure transmitter (DPT). The bubble size was obtained from the camera recordings of the experiment.

It was observed that longer Taylor bubbles reduce in size faster than smaller bubbles. There are two trends present in regards to the bubble decay rate: longer bubbles seem to decay linearly, while shorter bubbles decay exponentially. This is believed to be a consequence of two mechanisms that determine the decay rate: (a) the physical brake-up of the bubble at the bubble tail into smaller bubbles that get washed away with the flow, and (b) the dissolution of the gas phase into non-saturated liquid phase. The former mechanism is most prevalent in longer bubbles, but it slows down with the reduction of bubble length. Contrarily, the bubble dissolution is always present in non-saturated liquid; however, it is more significant for short bubbles. Subsequently, two sets of measurements were performed: one set for long and one for short bubbles in order to separate the two mechanisms.

1 INTRODUCTION

In a slug-type two-phase flow, large bullet-shaped gas structures occupy almost the entire cross-section of the flow channel, surrounded by a thin liquid film. These structures are often referred to as Taylor bubbles, which are separated by “slugs” of the liquid phase. The present study focuses on the stability study of a single Taylor bubble in a vertical counter-current flow configuration. Slug flows with Taylor bubbles are present in many industrial and technological applications, such as desalination systems, transportation of hydrocarbons, boiling and condensation systems in thermal power plants, and in the emergency core cooling of nuclear reactors during a Loss of Coolant Accident (LOCA).

It was observed that a Taylor bubble decays in size over time. The effect is believed to be a consequence of two different mechanisms: the physical break-up into smaller bubbles at the tail end of the Taylor bubble, and dissolution of the gas into the liquid phase [1]. However, state-of-the-art simulations of such two-phase flow still severely over predict the bubble decay rate [2][3], which represents a need for a detailed experimental investigation and better understanding of these processes. In the present study an attempt was made to separate the two mechanisms acting upon the bubble, which can lead to the development of better models for numerical simulations.

2 EXPERIMENTAL DEVICE AND INSTRUMENTATION

The measurements were performed using the experimental loop shown in Figure 1. The test section consists of a vertical glass pipe where the Taylor bubble can be observed visually. The test section is modular in order to accommodate different pipe diameters. In the case of this study, circular pipes with inner diameters of 12.4 and 26 mm were used. Water flow enters the test section from the top and is supplied by a centrifugal pump located below the section. Two regulation valves were used in order to control the mass flow rate of water through the test section. The first is located upstream of the test section and is used to control the amount of water flowing through the bypass loop and back to the tank. The second is located downstream of the test section and determines the flow rate exiting the section. Both valves also determine the pressure in the system.

A *Micro Motion CMFS025M* Coriolis flow meter was used in order to record the mass flow rate of the water. The flow meter has a mass flow rate measurement accuracy of ±0.1%. The temperature of the water was controlled and kept constant using a heat exchanger located in the water tank and recorded using a type-T thermocouple with an accuracy of ±1°C. The pressure was recorded using the *ABB 266AST* absolute pressure transmitter, while the pressure drop across the test section was also recorded using the *ABB 266MST* differential pressure transmitter. The sensors have a base accuracy of 0.04% of the measuring span, which corresponds to the absolute errors of ±160 Pa for the absolute pressure transmitter and about ±2 Pa for the differential pressure transmitter. The values were recorded at the frequency of 1 Hz. A *Logitech C920s HD Pro* web camera was used to record the bubble during the duration of the experiment.

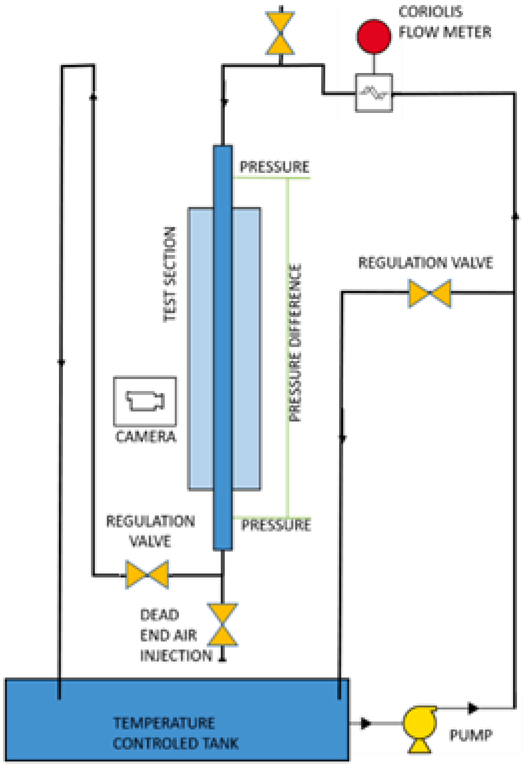

Figure 1: Scheme of the experimental device.

3 MEASUREMENT PROCEDURE

To perform an individual measurement, the test conditions had to be established. First, the desired temperature in the test section was reached using a thermal bath that heated or cooled the water in the tank via a heat exchanger. Next, the de-gasification valve positioned directly above the test section was opened in order to get rid of any gas present in the system from previous measurements. At this point, the bypass valves and outlet valve were adjusted in order to reach the required pressure and mass flow rate in the system.

The experiments were performed using argon gas. It was chosen due to its relatively large density, low solubility in water, as well as the fact that it is a pure gas that introduces only a single component, unlike air, which is a mixture of various gases each with different solubilities in water. The gas was introduced to the loop below the test section from a pressurized argon gas tank. The size of the bubble was determined by the amount of time the valve connecting the argon tank to the test section was left open. The gas took shape of a Taylor bubble inside the pipe and was allowed to rise into the desired position in the section by buoyancy. At this point, an adjustment of the mass flow rate of the water was performed, in order to achieve equilibrium between the counter-current water flow and the force of buoyancy, resulting in a stationary Taylor bubble. During the duration of the experiment, small manual adjustments to the mass flow rate were needed every few seconds in order to keep the bubble in the field of view of the camera used to record the experiment. This had a small effect on the mass flow rate of the water and absolute pressure in the system. It was calculated that the variations of the mass flow rate were between 3% and 10% of the mean flow rate. These fluctuations are roughly one order of magnitude larger than the flow rate fluctuations due to the turbulent nature of the single phase channel flow obtained in our Direct Numerical Simulation (DNS) studies at constant pressure gradient boundary conditions performed in computational domains that were around 5 hydraulic diameters long [4]. The inherent instability of the bubble is a consequence of factors such as interference from the environment, the chaotic nature of turbulent flow, imperfect operation of the pump, and related sources of interference.

The experiment was performed using two glass pipes with inner diameter of 12.4 mm and 26 mm. Each measurement was performed for short and long bubbles. Long bubbles started at lengths of 650-800 mm, which corresponds to a relative length of 25 to 30 hydraulic diameters for the thick pipe and 54 to 67 hydraulic diameters for the thin pipe. The experiments were concluded once the bubble decayed to about 300 mm. For the short bubbles, the starting lengths ranged from 60 to 80 mm for the thick pipe, corresponding to relative lengths of 2 to 3 hydraulic diameters and from 40 to 50 mm for the thin pipe, corresponding to 3 to 4 hydraulic diameters. For each combination of bubble length and pipe diameter a set of 16 measurements were performed at pressures of about 1, 1.5, 2 and 2.5 bar and temperatures of 20, 30, 40 and 50 °C. Each measurement lasted from 20 to 50 minutes depending on the conditions of the experiment. This resulted in a combined data set of 64 individual measurements, which are presented in Table 1, including the calculated average Reynolds number value for each measurement. The bubble was observed and recorded using a web camera situated about 1 m from the test section. The video was later analysed in order to obtain the lengths of the Taylor bubble at different times during the duration of the experiment. Lengths of the bubble were recorded at intervals of 30 or 60 s, depending on the decay rate of the Taylor bubble.

Table 1: Measurement matrix with the calculated average Reynolds number for each measurement.

Long bubble										
Thin pipe						Thick pipe				
	20°C	30°C	40°C	50°C			20°C	30°C	40°C	50°C
1 bar	1150	1450	1770	2080		1 bar	4540	5720	6950	8660
1.5 bar	1130	1430	1740	2080		1.5 bar	4810	5660	7150	8700
2 bar	1130	1470	1810	2190		2 bar	4870	5680	7220	8510
2.5 bar	1140	1460	1770	2120		2.5 bar	4820	5860	7420	8550
Short bubble										
Thin pipe						Thick pipe				
	20°C	30°C	40°C	50°C			20°C	30°C	40°C	50°C
1 bar	1200	1450	1750	2060		1 bar	4600	5540	6820	8080
1.5 bar	1150	1480	1830	2070		1.5 bar	4740	5670	7110	8470
2 bar	1160	1450	1760	2090		2 bar	4880	5680	6810	8430
2.5 bar	1170	1510	1850	2220		2.5 bar	5040	5800	7090	8380

4 RESULTS

The results from individual measurements were plotted and analysed. Plots showing the bubble length with respect to time were produced and a linear approximation curve was fitted for each measurement. Since the entire duration of the measurement does not display a linear trend, only selected data points were chosen for the curve fit. An example of a plotted measurement and the fitted linear curve is shown on Figure 2.

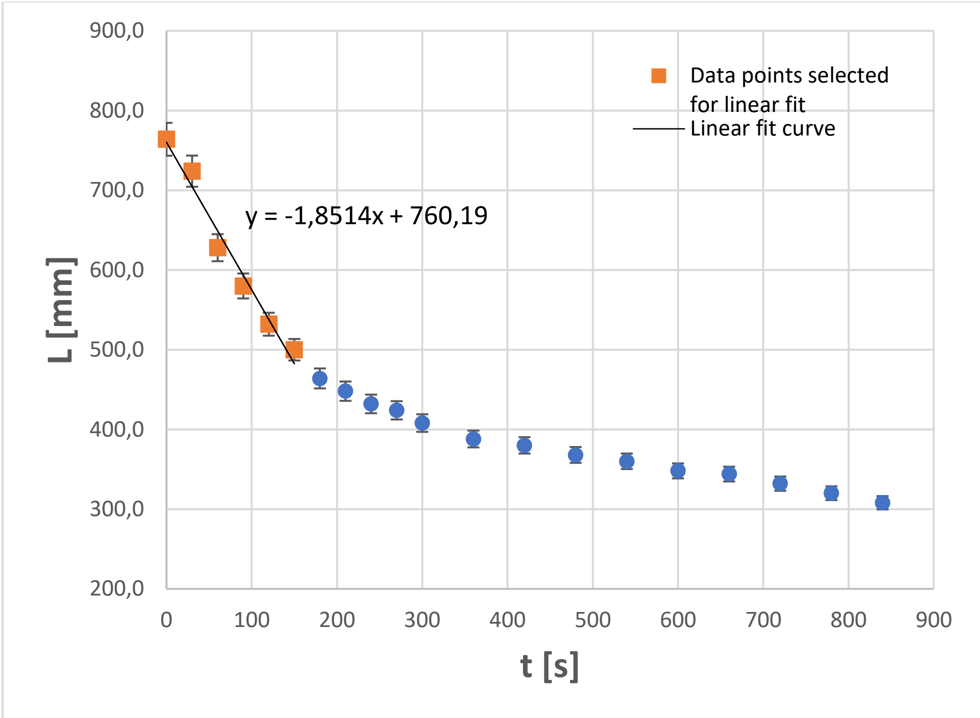

Figure 2: Example of the bubble decay rate for a single measurement and the fitted linear function (long bubble, thick pipe, 1 bar, 40°C)

The coefficients of the curves (*k*) represent the decay rate of the bubble. They were recorded and plotted as contour graphs with respect to pressure and temperature, shown in Figure 3.

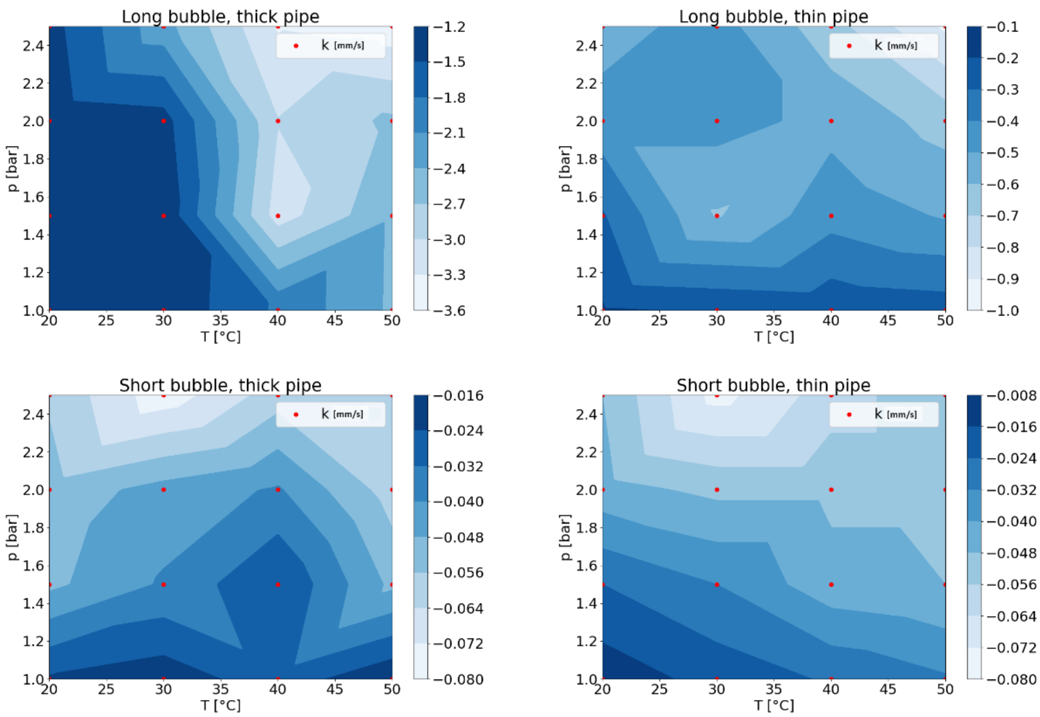

Figure 3: Contour graphs showing the values of fitted linear curves coefficients (i.e. bubble decay rates) with respect to pressure and temperature

It was noted that large bubbles decay much faster in size than small bubbles. It is visually observed that large bubbles break-up at the tail end into smaller bubbles, which can get washed away in the flow of water. This is not present in smaller bubbles, thus, the fast bubble decay can be attributed to the highly turbulent flow at the tail end of a large Taylor bubble, which causes bubble breakup. Contrarily, small bubbles decay slowly, which is usually attributed to the dissolution of the gas into the liquid phase [1]. Regardless the size of the Taylor bubble, Figure 3 shows that the decay rate of the bubbles increases with the increase of temperature and pressure, with pressure having a more significant effect.

At first glance, the experimental results of this study might seem counter-intuitive, as one can see that the decay rate of the bubbles increases with temperature increase. This may seem in contradiction with the fact that the solubility of argon in water decreases with temperature increase [5]. However, one must also take into consideration the change in Reynolds number, which increases with temperature increase (as seen in Table 1), thus making the flow more turbulent, which causes a higher rate of break-up of the bubble. The trend however is relatively weak compared to the effect of pressure. It is evident that with an increase of absolute pressure in the system, the decay rate increases. This is in accordance with the fact that the argon solubility into the liquid phase increases with pressure increase.

Different decay rates were also observed for the different pipe diameters, with the decay rate being larger in the thicker pipe. This fact is again believed to be tied to the Reynolds number, as the values in the thick pipe indicate a turbulent flow (4500-8800) and are considerably larger than the values in the thin pipe (1100 – 2200), where laminar flow is present. This had an observable effect on the Taylor bubble itself: the bubbles in the thin pipe were more axisymmetric and stable, requiring fewer manual adjustments in order to keep the bubble in the field of view of the camera. The bubbles in the large pipe tended to have a more irregular shape, tilted towards the wall of the pipe, with the liquid film around the bubble being thicker on one side than the other. This effect has been observed and analysed by Kren et. al. [6].

Figure 3 shows a 3D graph of the coefficients in which a linear plane was fitted to the measurements. The fitting function used to construct the plane was as follows:

$$f(T, p) = aT + bp + c \tag{1}$$

Here, *a*, *b* and *c* are the slope coefficients, which can be found in Table 2 along with their respective asymptotic standard errors. *T* represents temperature in °C and *p* represents pressure in bar.

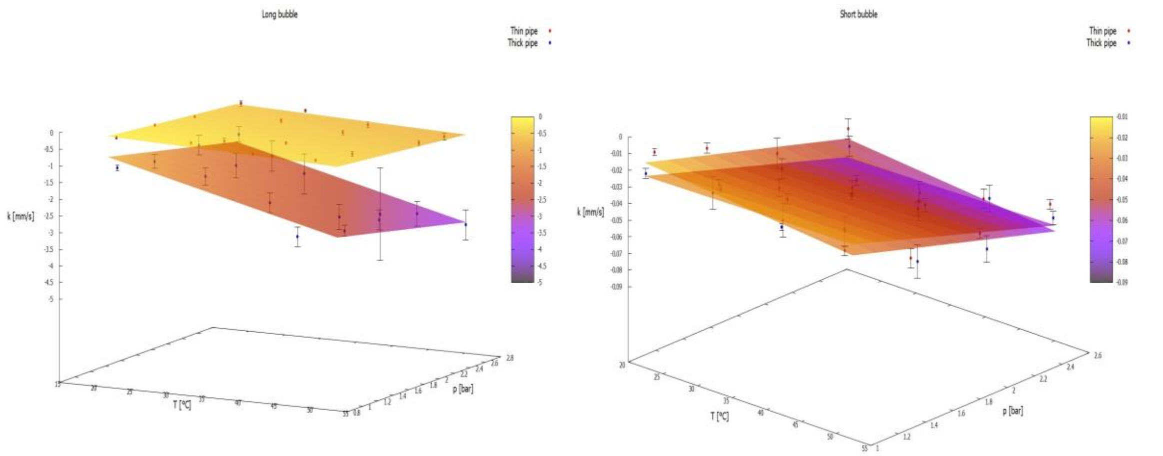

Figure 3: 3D graphs showing the planes fitted to the values of linear coefficients with respect to pressure and temperature

Table 2: Slope coefficients and respective asymptotic standard errors

	a	b	c
Long bubble			
Thin pipe	-0.007 ± 0.002 **(30%)**	-0.3 ± 0.04 **(20%)**	0.2 ± 0.1 **(50%)**
Thick pipe	-0.05 ± 0.01 **(20%)**	-0.6 ± 0.2 **(40%)**	0.9 ± 0.5 **(60%)**
Short bubble			
Thin pipe	$-4.2 \times 10^{-4} \pm 1.8 \times 10^{-4}$ **(40%)**	-0.025 ± 0.004 **(15%)**	0.02 ± 0.01 **(50%)**
Thick pipe	$6.6 \times 10^{-5} \pm 2.2 \times 10^{-4}$ **(30%)**	-0.027 ± 0.004 **(15%)**	0.003 ± 0.01 **(400%)**

It can be observed that the standard asymptotic error ranges from 15% to 40% for the parameters *a* and *b*, which correspond to temperature and absolute pressure, respectively. The errors for the *c* parameter tend to be somewhat larger, ranging from 50% to 60%. However, the *c* parameter only determines the height of the plane and not its slope, and is therefore not as important to consider. The set of measurements for the short bubble in a thick pipe stands out because of its large error, which should be taken into account when drawing conclusions from the data.

5 CONCLUSION

The decay rate of a Taylor bubble has been observed in a laminar and turbulent flow regime at different temperatures and absolute pressures. We have reached the following conclusions:

- The decay rate increases as pressure and temperature increase. The effect of pressure is quite significant, while the correlation with temperature is problematic, as the Reynolds number varies substantially between individual measurements. This also influences the decay rate, making isolating the effect of temperature difficult.
- The strong pressure dependence of the decay rate can be attributed to the dissolution of argon into the liquid water phase. The solubility of argon increases with pressure, while the Reynolds number stays roughly constant.
- The rate of dissolution appears to be constant in both pipe diameters, and is therefore independent of the Reynolds number. On the other hand, the physical break-up of the Taylor bubble at the tail end is highly dependent on the flow regime – a higher Reynolds number causes the rate of break-up to increase.

ACKNOWLEDGMENTS

The authors gratefully acknowledge financial support provided by Slovenian Research Agency, grants P2-0026 and NC-0026.

REFERENCES

[1] B. Mikuž, J. Kamnikar, J. Prošek, I. Tiselj, "Experimental Observation of Taylor Bubble Disintegration in Turbulent Flow". Proc. Int. Conf. Nuclear Energy for New Europe 2019, Portorož, Slovenia, September 9-12 2019, pp. 211.1-211.8.

[2] E. Frederix, B. Mikuž, E. Komen, "LES of a Taylor bubble in co-current turbulent pipe flow". Direct and Large Eddy Simulation 12 - DLES12, Madrid, Spain, 5-7 June, 2019.

[3] B. Mikuž, E. Frederix, I. Tiselj, E. Komen, “High-fidelity simulation of a Taylor bubble in co-current turbulent flow”. Proceedings of 18th International Topical Meeting on Nuclear Reactor Thermal Hydraulics - NURETH, Portland, Oregon, US, 18-23 August 2019.

[4] R. Bergant, I. Tiselj, “Near-wall passive scalar transport at high Prandtl numbers”. Physics of Fluids, 19(6), 2007, 065105

[5] Rolf Sander: “Henry’s Law Constants (Argon)”. NIST Chemistry WebBook, SRD 69, Eds. P.J. Linstrom and W.G. Mallard, National Institute of Standards and Technology, Gaithersburg MD, 20899, (retrieved August 19, 2023). [Online]. Available: https://webbook.nist.gov/cgi/cbook.cgi?ID=C7440371&Mask=10

[6] J. Kren, B. Zajec, I. Tiselj, S. El Shawish, Ž. Perne, M. Tekavčič, B. Mikuž, “Dynamics of Taylor Bubble Interface in Vertical Turbulent Counter-current Flow”. Int. J. of Multiphase Flow, 165, 2023, 104482